Supporting Information

Environmentally Fluorine-free Sandwich Coating Based on Nonwoven Fabric for Efficient Unidirectional Water Transport

Songnan Zhang[a], Shuhua Li[a], Zhibin Zhang[a], Jianying Huang[b], Yuekun Lai *[b], Yan Feng*[a], Xiaoming Qian[a]*

[a] State Key Laboratory of Separation Membranes and Membrane Processes/ National Center for International Joint Research on Separation Membranes, School of Textile Science and Engineering, Tiangong University, Tianjin 300387, P. R. China

[b] National Engineering Research Center of Chemical Fertilizer Catalyst (NERC-CFC), College of Chemical Engineering, Fuzhou University, Fuzhou 350116, P. R. China

***Corresponding Author:**

Tel.+86-138-21367059

Email address: zhangsongnan@tiangong.edu.cn (*Songnan Zhang*)

yklai@fzu.edu.cn (*Yuekun Lai*)

fengyan@tiangong.edu.cn (*Yan Feng*)

Experimental

Materials

Methyltrimethoxysilane (MTMS) and oxalic acid were purchased from Shanghai Macleans Biochemical Technology Co., Ltd. Polydimethylsiloxane (PDMS, Sylgard 184: silicone elastomer and silicone elastomer curing agent) was produced by Shenzhen Taodu Technology Co., Ltd. Methanol, ammonium hydroxide (25%-28%) and tetra methylene oxide (THF) were purchased from Tianjin Komiou Chemical Reagent Co., Ltd. Viscose spunlace nonwoven fabric was provided by Lang fang Donglun Technology Industrial Co., Ltd. All the reagents were of analytical grade.

Preparation of ormosil

Ormosil was prepared under normal temperature and pressure conditions through sol-gel method. Firstly, oxalic acid (0.6 mL, 0.001 M) was added to the MTMS solution diluted with methanol and stirred for 30 min to make it fully hydrolyzed for 24 h. In this process, the precursor MTMS underwent a hydrolysis reaction under acidic conditions. Secondly, After the hydrolysis, 0.5 mL of ammonia water and 0.1 mL of distilled water were slowly added as a catalyst, and stirred for 30 minutes to cause the condensation reaction. In this process, it underwent a series of condensation reactions under the action of the catalyst ammonia, including dealcoholization condensation, dehydration condensation, and mutual condensation between small silica colloidal particles. Thirdly, in order to make the gel shape well and the pore structure complete, it needed to take 48 hours of standing aging to form a silicone gel[1, 2]. Finally, after the aging was over, diluted with 30 mL methanol and then ultrasonically dispersed for 30

min to obtain the uniform dispersed ormosil solution.

Preparation of PDMS coating

The ratio of 10:1 was used to formulate PDMS (0.5 mL silicone elastomer and 0.05 mL silicone elastomer curing agent). After mixing, the solution was diluted with 60 mL of tetra methylene oxide, stirred for 30 minutes, and ultrasonically dispersed for 30 minutes to obtain the uniform dispersed solution.

Fabrication of Janus nonwoven fabric

Preparation of ormosil@ NF

In order to increase the surface roughness, the ormosil solution was prepared and sprayed on the NF surface. The untreated nonwoven fabric was fixed flatly on the board with a spraying distance of 12 cm, then was sprayed with a volume of 2.5 mL ormosil solution. Subsequently, it was dried in an oven at 60 °C for 2 h. The ormosil particles loaded on the NF could not only improve the surface roughness, but also possess a certain degree of hydrophobicity due to the formed three-dimensional -Si-O-Si- network structure which was surrounded by a large number of low-surface methyl groups ($-CH_3$).

Preparation of PDMS@ NF

PDMS, the low surface energy substance, which was environmentally friendly and had a certain viscosity, was selected to reduce the surface energy of the nonwoven fabric surface and make it hydrophobic. The untreated nonwoven fabric was fixed flatly on the board with a spraying distance of 12 cm, and then was sprayed with a volume of 6 mL PDMS solution. Subsequently, it was dried in an oven at 60°C for 2 h.

Preparation of PDMS-ormosil-PDMS@ NF

Firstly, the untreated nonwoven fabric was fixed flatly on the board with a spraying distance of 12 cm, and was sprayed with a volume of 3 mL PDMS solution, which was to construct a hydrophobic bonding layer and make the following ormosil particles better adhere to the NF surface. Secondly, followed by spraying the ormosil solution with a volume of 2.5 mL in order to construct rougher surface and strengthen the hydrophobic property. Finally, followed by spraying a second PDMS layer with a volume of 3 mL, which was to enhance the hydrophobicity, adhesion and mechanical stability of the surface. Subsequently, it was dried in an oven at 60 °C for 2 h.

Characterization

The surface morphology and chemical element distribution of the samples were characterized by scanning electron microscopy（SEM，Phenom XL，Netherlands） and energy dispersive X-ray spectrometer (EDS), respectively. The surface roughness of the sample was tested and analyzed with a true color confocal microscope (Zeiss CSM700, ZEISS, Germany). The chemical composition of the sample surfaces was characterized by Fourier transform infrared (FTIR) spectroscopy (Nicolet iS50, Thermo Fisher Scientific) and X-ray photoelectron spectroscopy (XPS, K-alpha, Thermofisher), respectively. In addition, the contact angle meter (KRUSS DSA100, Germany) was used to test the wettability of water droplets (1 μL) on the sample surface and record the dynamic penetration process of water droplets (1 μL). The water directional transportation behavior of Janus nonwoven fabrics was characterized by the water management tester (MMT). According to the standard ISO 8251-87, a sandpaper

abrasion test was carried out to characterize the abrasion stability of the sample surface. The thickness and air permeability of the samples were tested using a thickness gauge and YG461H full-automatic air permeability meter, respectively.

Supplementary figures

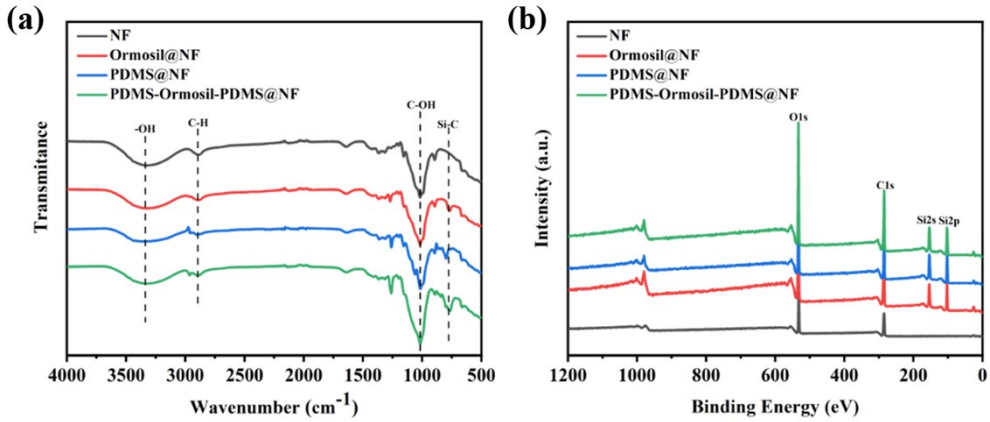

Fig. S1 a) FTIR and b) XPS spectra of hydrophobic side of untreated NF, ormosil@ NF, PDMS@ NF, PDMS-ormosil-PDMS@ NF.

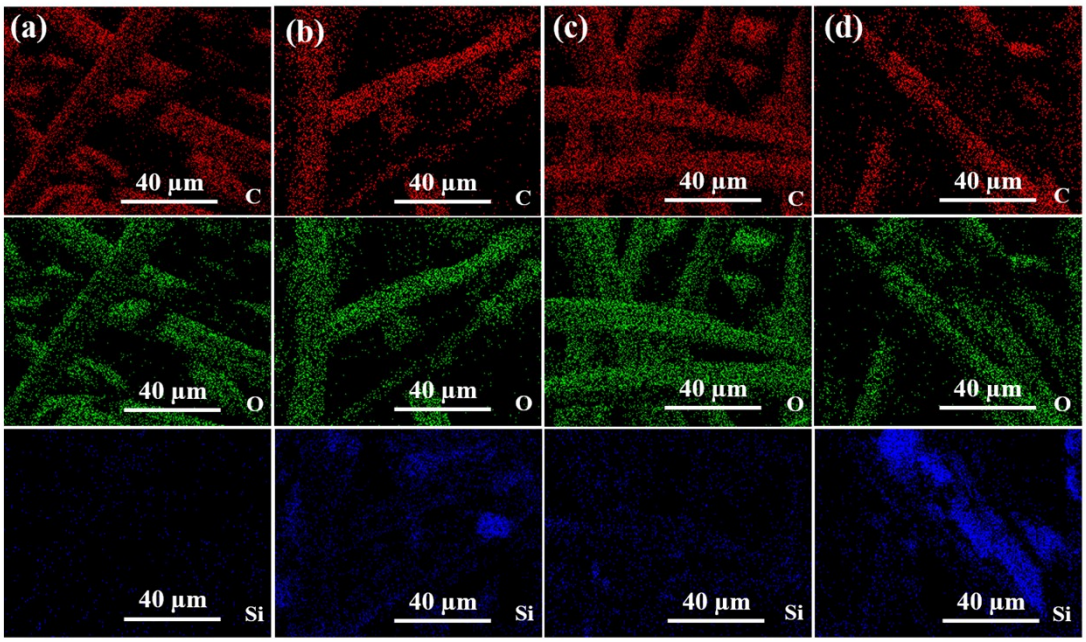

Fig. S2 Element mapping and EDS spectrum of a) untreated NF, b) ormosil@ NF, c) PDMS@ NF, d) PDMS-ormosil-PDMS@ NF.

Table S1 Corresponding to the content of C, O and Si elements in the EDS spectrum

NF	NF		ormosil@ NF		PDM@ NF		PDMS-ormosil-PDMS@ NF	
Element	Wt%	At%	Wt%	At%	Wt%	At%	Wt%	At%
C	47.95	55.10	46.06	55.06	47.16	54.63	42.34	53.58
O	52.00	44.87	44.94	40.34	51.26	44.58	37.21	35.35
Si	00.05	00.03	09.00	04.60	01.59	00.79	20.45	11.07

Fourier transform infrared (FTIR) spectroscopy, X-ray photoelectron spectroscopy (XPS) and energy dispersive X-ray spectrometer (EDS) were used to characterize the surface chemical composition and elements distribution of Janus nonwoven fabrics. In the infrared spectrum (**Fig. S1a**), the viscose spunlace nonwoven fabric had strong absorption peaks at the stretching frequency of 3250-3500 cm^{-1}, 2750-3000 cm^{-1} and 1000-1100 cm^{-1}, corresponding to -OH, C-H and C-OH functional groups, respectively. The strong absorption peak of Si-C (750-850 cm^{-1}) had been added to the spectra after ormosil and PDMS processing, which proved the success of ormosil@ NF, PDMS@ NF and PDMS-ormosil-PDMS@ NF synthesis. X-ray photoelectron spectroscopy (XPS) was used to further study and analyze the surface element composition of Janus nonwoven fabrics (**Fig. S1b**). Nonwoven fabrics were composed of carbon and oxygen. After the treatment with ormosil and PDMS, the XPS spectrum showed strong signals of Si2s and Si2p, proving the successful synthesis of ormosil@ NF, PDMS@ NF and PDMS-ormosil-PDMS@ NF. As shown in **Fig. S2a-d**, the energy dispersive X-ray spectrometer (EDS) was used to observe and analyze the distribution and content of each elements, mainly scanning and testing three elements, viz. C, O, Si, thereinto each color represented an element. As shown in **Fig. S2a**, there

was almost no Si element distribution on the surface of the untreated nonwoven fabric. Results revealed that the distribution content of Si element on the NF surface treated with ormosil and PDMS gradually increased, and the distribution content of PDMS-ormosil-PDMS@NF was the most (**Table 1**), which was also consistent with the results of FTIR and XPS spectroscopy, and both proved the successful combination of ormosil and PDMS coating on the NF surface.

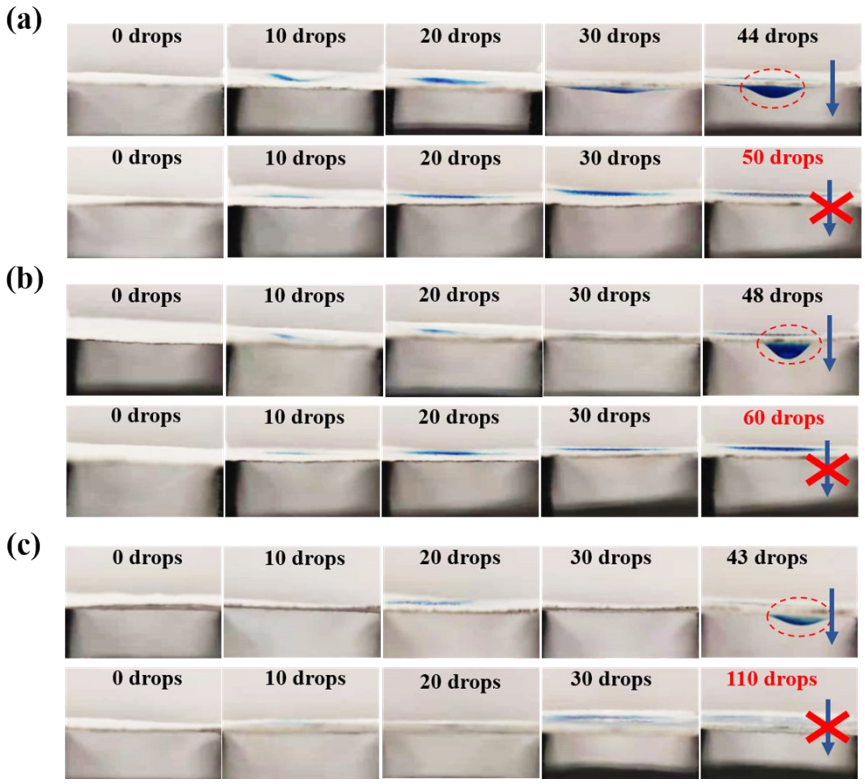

Fig. S3 a-c) Water droplets can transport from the hydrophobic side to the hydrophilic side, cannot transport from the hydrophilic side to the hydrophobic side until reaching the limit, a) ormosil@ NF, b) PDMS@ NF, c) PDMS-ormosil-PDMS@ NF, the volume of each drop is 1 mL.

To verify and analyze the unidirectional water transport behavior of three different samples, we further observed the dynamic behavior as shown in **Fig. S3a-c**, the water

droplets of 1 mL size were fixed and maintained each time. As for three samples, when droplets were dripped onto the hydrophobic side, the penetration phenomenon could instantly happen. In contrast, the penetration phenomenon could not happen when droplets were dripped onto the hydrophilic side until reaching the limit. The limit for ormosil@ NF, PDMS@ NF and PDMS-ormosil-PDMS@ NF were 50, 60, 110 drops, respectively. Results revealed that Janus hydrophilic/hydrophobic composite infiltration gradient would benefit for water droplets transporting from the hydrophobic side to the hydrophilic side successfully. In the reverse transportation, the water droplets would be blocked by this gradient force. As for PDMS-ormosil-PDMS@ NF, the limit showed the best, indicating the highest osmotic pressure, which proved the best unidirectional water transport performance of Janus nonwoven fabrics.

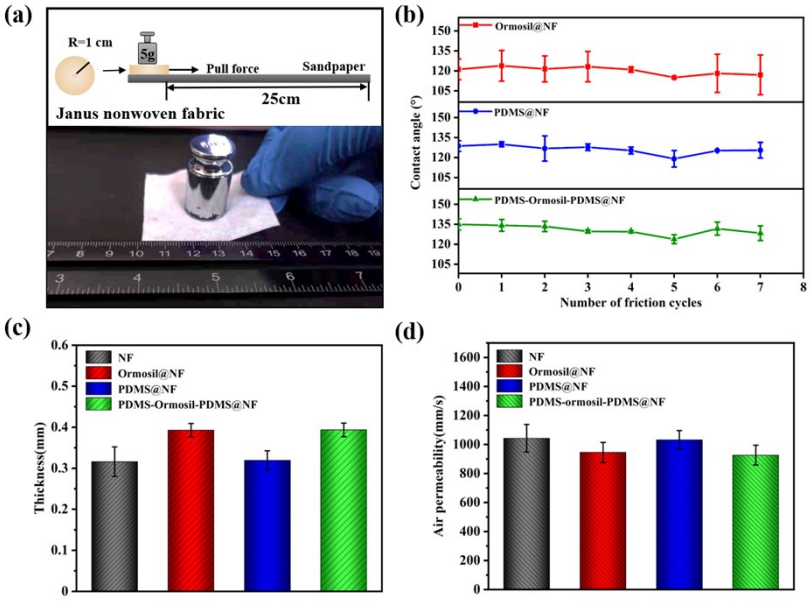

Fig. S4 a) Schematic illustration of friction resistance. b) Contact angle of 7 friction cycles of ormosil@ NF, PDMS@ NF, PDMS-ormosil-PDMS@ NF. The surface hydrophobicity was still stable after friction, PDMS-ormosil-PDMS@ NF had the best

hydrophobic performance. c) Variation in thickness of NF. d) Air permeability change of NF.

As shown in **Fig. S4a**, 1000 mesh sandpaper and a weight of 5 g were used to carry out the sandpaper abrasion experiment. The mechanical abrasion cycle was defined as a parallel pulling 25 cm, and the Janus nonwoven fabrics test sample was a circle with a radius of 1 cm. Through testing the change of contact angle after each mechanical abrasion, we found that the samples treated in three ways could still maintain a relatively stable hydrophobic performance as shown in **Fig. S4b**. In general, after seven sandpaper abrasion tests, the contact angle of ormosil@ NF, PDMS@ NF and PDMS-ormosil-PDMS@ NF were stable at about 120°, 126° and 133°, respectively. But as the number of abrasion cycles increased, the error analysis in the figure showed that the hydrophobic stability of ormosil@ NF and PDMS@ NF were worse than PDMS-ormosil-PDMS@ NF after sandpaper abrasion, which proved that the PDMS-ormosil-PDMS@ NF had the best hydrophobic stability effect.

Besides, we further studied and compared the thickness and air permeability before and after the treatment. By comparison, we found that the thickness difference among the untreated NF, ormosil@ NF, PDMS@ NF and PDMS-ormosil-PDMS@ NF was small as shown in Figure 8c, between tens of microns as well as the air permeability difference. Generalized analysis from **Fig. S4c-d**, we found that the air permeability would be not better than ever when their thickness increased, which indicated that the thickness would not benefit for the air permeability. Even though the adhesion of ormosil particles and PDMS coating on the surface would reduce the porosity of the

surface of the nonwoven fabric, the difference in air permeability was overall small and still maintained in a good state.

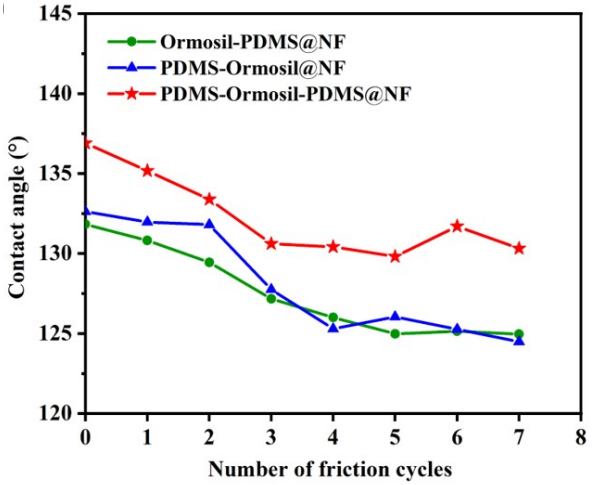

Fig. S5 Contact angle of 7 friction cycles of ormosil-PDMS@ NF, PDMS-ormosil@ NF, PDMS-ormosil-PDMS@ NF. The surface hydrophobicity was still stable after friction, PDMS-ormosil-PDMS@ NF had the best hydrophobic performance.

In the previous experimental work, we tried to prepare ormosil-PDMS@ NF and PDMS-ormosil@ NF for comparative testing. But after the sandpaper abrasion test as shown in Fig. S4a, their surface hydrophobicity and mechanical friction resistance was worse (Figure S5) compared to PDMS-ormosil-PDMS@ NF.

Table S2 Summary of other relevant work reported

References	Materials	Contact angle（°）	One-way transportation capacity(R%)
3	fibrous membranes	128°	1021%
4	composite fibrous mat	119°	870%
5	1D fiber assemblies	135°	1034.5%
6	fibrous membranes	137°	297%
7	porous membrane	—	960.76%
8	Composite membranes	128.6°	1253%
9	composite yarn	121.3°	400.9%
This work	**composite nonwoven fabric**	**137°**	**907.09%**

Nowadays, fewer studies are reported about unidirectional water transport on nonwoven fabrics, whereas most of reports mainly focused on membrane materials or wowen fabrics. Zhang et al .[10] prepared a Janus composite electrospun membrane with directional water transport properties. They prepared hydrophobic thermoplastic polyurethane (TPU) and super-hydrophilic polyacrylonitrile (PAN) using electrospinning method, then applied a layer of dopamine (DPA) on the PAN layer to adjust the wettability of the composite film. After utlizing a fully automatic air permeability measuring instrument, they characterized the air permeability of the composite membrane and found that the optimal air permeability was about 125 mm/s. Additionally, Zou et al. [7] laminated the prepared cellulose acetate/blends of polyvinyl alcohol and polyacrylic acid (CA/PA) bilayer porous membrane on a polyester fabric and applied it in the field of directional water transportation. The test and characterization showed that the optimal air permeability value of this composite material was 382.76 mm/s.

Reference

1. X. Zhang, M. Lin, L. Lin, M. Zhuang, L. Ye, W. Yang and B. Jiang, *J. Sol-Gel Sci. Techn.*, 2015, **74**, 698-706.
2. T. L. Metroke, O. Kachurina and E. T. Knobbe, *Prog. Org. Coat.*, 2002, **44**, 295-305.
3. D. Miao, Z. Huang, X. Wang, J. Yu and B. Ding, *Small* 2018, **14**, 1801527
4. J. H. Xu, F. L. Zhang, B. J. Xin, C. Wang, D. Yang, Y. S. Zheng and M. J. Zhou, *Polym. Advan.Technol.*, 2019, **30**, 3038-3048.

5. N. Mao, H. Peng, Z. Z. Quan, H. N. Zhang, D. Q. Wu, X. H. Qin, R. W. Wang and J. Y. Yu, *ACS Appl. Mater. Inter.*, 2019, **11**, 44682-44690.

6. S. N. Tang, H. H. Pi, Y. Y. Zhang, J. Wu and X. Q. Zhang, *Appl. Sci.-Basel*, 2019, **9**, 9163302.

7. F. W. Zou, Y. Q. Dong, M. H. Wang, H. Sliman, X. F. Wang and T. Zhao, *Fiber. Polym.*, 2021, **22**, 2404-2412.

8. A. A. Babar, X. L. Zhao, X. F. Wang, J. Y. Yu and B. Ding, *J. Colloid Interf. Sci.*, 2020, **577**, 207-216.

9. N. Mao, X. H. Qin, L. M. Wang and J. Y. Yu, *Text. Res. J.*, 2021, **91**, 1467-1477.

10. Y. Zhang, T. T. Li, H. T. Ren, F. Sun, Q. Lin, J. H. Lin and C. W. Lou, *RSC Adv.*, 2020, **10**, 3529-3538.